Correcting atmospheric CO_2 and CH_4 mole fractions obtained with Picarro analyzers for sensitivity of cavity pressure to water vapor

Friedemann Reum[1], Christoph Gerbig[1], Jost V. Lavric[1], Chris W. Rella[2] and Mathias Göckede[1]

[1]Max Planck Institute for Biogeochemistry, Jena, Germany
5   [2]Picarro Inc., Santa Clara, CA, USA

Correspondence to: Friedemann Reum (freum@bgc-jena.mpg.de)

Abstract. Measurements of dry air mole fractions of atmospheric greenhouse gases are used in inverse models of atmospheric tracer transport to quantify their sources and sinks. The measurements have to be calibrated to a common scale to avoid bias in the inferred fluxes. For this purpose, the World Meteorological Organization (WMO) has set requirements
10   for the inter-laboratory compatibility of atmospheric greenhouse gas (GHG) measurements. A widely used series of devices for these measurements are the GHG analyzers manufactured by Picarro, Inc. These are often operated in humid air, and the effects of water vapor are corrected for in post-processing. Here, we report on rarely detected and previously unexplained biases of the water correction method for CO_2 and CH_4 in the literature. They are largest at water vapor mole fractions below 0.5 % H_2O, which were undersampled in previous studies, and can therefore affect measurements obtained in humid air and
15   in air dried with a Nafion membrane. The biases, which can amount to considerable fractions of the WMO goals, are caused by a sensitivity of the pressure in the measurement cavity to water vapor. We correct these biases by modifying the water correction method from the literature. Our method relies on experiments that maintain stable water vapor levels to allow equilibration of cavity pressure. The commonly used droplet method does not fulfill this requirement. Correcting CO_2 measurements proved challenging, presumably because of our humidification method. Open questions pertain to differences
20   between analyzers and variability over time. Correcting the cavity pressure-related biases helps keeping the overall accuracy of measurements of dry air mole fractions of CO_2 and CH_4 obtained with Picarro GHG analyzers in humid and Nafion-dried air within the WMO goals.

1   Introduction

Measurements of atmospheric GHG mole fractions are integral data for quantifying their sources and sinks using inverse
25   models of atmospheric transport (e.g. Kirschke et al., 2013; McGuire et al., 2012). Inverse models require atmospheric measurements calibrated to a common scale, because relative biases in the atmospheric mole fractions lead to biases in the inferred fluxes. To ensure the high quality of greenhouse gas observations required for inverse models of atmospheric transport, the World Meteorological Organization (WMO) has set compatibility goals for atmospheric CO_2 and CH_4 measurements to ±0.1 ppm for CO_2 (±0.05 ppm in the southern hemisphere) and ±2 ppb for CH_4 (WMO, 2016). Models of

atmospheric greenhouse gas transport require dry air mole fractions as input, i.e. the number of molecules of the target gas divided by the number of air molecules excluding water vapor. Water vapor is excluded because its variability would mask signals in the greenhouse gases.

GHG analyzers manufactured by Picarro Inc. (Santa Clara, CA), which are based on the cavity ring-down spectroscopy technique (Crosson, 2008), are used at many sites of the international GHG monitoring network because of their signal stability. Due to limitations of air sample drying techniques (Rella et al., 2013), these analyzers are often operated in humid air, and dry air mole fractions are obtained by correcting for the effects of water vapor in a post-processing step (Chen et al., 2010; Rella et al., 2013). The effect of water vapor on trace gas readings can be described by a water correction function $f_c(h)$, where c denotes the target gas (here: CO_2 or CH_4) and h is the water vapor mole fraction (measured by the Picarro analyzer). The analyzer reports wet air mole fractions $c_{wet}(h)$, from which dry air mole fractions c_{dry} can be obtained by dividing by the water correction function:

$$c_{dry} = \frac{c_{wet}(h)}{f_c(h)} \tag{1}$$

The water correction function from the literature takes into account dilution and line shape effects. These are described by a second-degree Taylor series, i.e. a parabola (Chen et al., 2010; Rella et al., 2013):

$$f_c^{para}(h) = 1 + a_c \cdot h + b_c \cdot h^2 \tag{2}$$

Thus, dry air mole fractions based on this model are calculated as:

$$c_{dry}^{standard} = \frac{c_{wet}(h)}{f_c^{para}(h)} \tag{3}$$

Henceforth, we call this the "standard" water correction model.

In many previous studies featuring water corrections for CO_2 and CH_4, water vapor mole fractions below 0.5 % H_2O were only scarcely sampled (Chen et al., 2010; Nara et al., 2012; Rella et al., 2013; Winderlich et al., 2010). In this paper, we report on biases in $c_{dry}^{standard}$ in this domain that were not detected in these previous studies. They were, however, recently detected in one other study in which this domain was sufficiently sampled (Stavert et al., 2018). We characterize these biases, link them to an as yet undocumented sensitivity of the pressure inside the measurement cavity to water vapor, provide an approach to correct them, and discuss remaining challenges.

2   Materials and Methods

To determine the effect of water vapor on CO_2 and CH_4 measurements obtained using Picarro analyzers, as well as on the pressure in the measurement cavity, so-called "water correction" experiments similar to those in the literature (e.g. Rella et al., 2013) were performed, i.e. dry air from pressurized gas tanks was humidified and measured with Picarro GHG analyzers. Dry air mole fractions used were in the ranges 352–426 ppm CO_2 and 1797–2115 ppb CH_4. The key modification to the experiments in the literature was to monitor cavity pressure independently of the internally mounted cavity pressure sensor.

Atmospheric
Measurement
Techniques
Discussions

The setup varied between experiments (Table 1, Fig. 1–Fig. 3). Experiments were performed with five Picarro GHG analyzers, henceforth labeled "Picarro #1 – #5", and one Picarro oxygen analyzer labeled "Picarro #6" (Table 1). In the following sections, we first describe relevant aspects of the measurement principle and hardware of Picarro analyzers, and then describe our experiments.

5

Table 1: Overview of Picarro analyzers used in and experiments performed for this study.

Label	Picarro analyzer model	Picarro analyzer type	Droplet experiment with external pressure measurement	Stable H_2O level experiment: external cavity pressure measurement / usable trace gas measurements (reason)	Spectroscopic cavity pressure measurements
#1	G2401-m	Flight-ready	Yes	Yes / No (used ambient air)	No
#2	G2401	Regular	No	Yes / No (disregarded equilibration)	No
#3	G2401-m	Flight-ready	No	Yes / Yes	No
#4	G2401-mc	Flight-ready	No	No (before cavity pressure hypothesis was developed) / Yes	No
#5	G2301	Regular	No	No (remote field site) / Yes	No
#6	G2207-i	Regular	No	No	Yes

2.1 Picarro GHG analyzers: measurement principle and active cavity pressure stabilization system

Picarro GHG analyzers are based on the cavity ring-down spectroscopy method (Crosson, 2008). In a measurement cavity,
10 laser pulses scan absorption lines of the target gases. The time it takes the pulses to attenuate is converted to mole fractions of the gases. Among other requirements, the analysis assumes stable pressure inside the measurement cavity. Cavity pressure stability is achieved by a feedback loop (e.g. Fig. 1) between a pressure sensor (General Electric NPC-1210) that is mounted inside the cavity, and the outlet valve of the cavity (inlet valve in so-called flight-ready Picarro GHG analyzers, which are customized for airborne measurements). This loop keeps readings of the cavity pressure sensor stable. Picarro GHG
15 analyzers for CO_2 and CH_4 used in this study, i.e. model series G2301 and G2401, operate at 186.65 hPa (140 Torr) with a 1σ tolerance of 0.20 hPa.

2.2 Setups for humidification

To humidify the air stream, two different methods were used. The first approach was designed to maintain stable water vapor levels, while the second approach was the commonly used droplet method. In this section, we describe the experimental
20 setup for both methods.

2.2.1 Stable water vapor levels

To create an air stream with stable water vapor levels, the dry air stream was split into two lines, one of which remained untreated. Air in the other line was directed through a gas washing bottle that contained deionized water (e.g. Fig. 1). For experiments where CO_2 and CH_4 data were analyzed, the amount of water used was 15 ml (Picarro #3) or 40 ml (Picarros #4

5   and #5). With this method, air in the humidified line was saturated with water vapor (mole fraction ~3 % H_2O). In an experiment with Picarro #1, instead of using the gas washing bottle approach, stable water vapor levels were realized by mixing air from the gas tank with ambient laboratory air (CO_2 and CH_4 readings from this experiment were not analyzed). Subsequently, the two lines were joined again. The water vapor mole fraction in the re-joined line was controlled by adjusting the flow through the wet and dry lines. In the experiments with Picarros #1–#5, this was achieved using needle

10   valves; in the experiment with Picarro #6, mass flow controllers (Alicat Scientific, Tucson, Arizona) were used.

2.2.2 Droplet method

For droplet experiments, the humidification unit described above was replaced with a tee piece that enabled injecting water droplets into the dry air stream (Fig. 2).

2.3 Setups for cavity pressure monitoring

15   We used two methods to monitor pressure inside the measurement cavity independently of the internally mounted pressure sensor. The first method was based on an additional pressure sensor. Due to the complexity of this setup, we developed a second cavity pressure monitoring method, based on spectroscopic measurements, to verify the results of the first approach. In this section, we describe the experimental setups for both methods.

2.3.1 Cavity pressure monitoring with external sensor

20   For this approach, an additional pressure sensor (General Electric Druck DPI 142) was installed outside of the Picarro analyzer (e.g. Fig. 1). Since the external pressure sensor may itself be sensitive to water vapor, it was shielded from humidity changes by installing it behind a drying cartridge filled with magnesium perchlorate in a dead end. The external pressure measurement line was branched directly upstream of the Picarro GHG analyzer (downstream for flight-ready analyzers). To ensure that the external sensor could react to changes in cavity pressure, pressure in this branch was adjusted to within a few

25   hPa of cavity pressure by installing a needle valve as a choke upstream of the external pressure measurement branch (downstream for flight-ready analyzers). This setup allowed monitoring cavity pressure independently of water vapor content, while the internal cavity pressure sensor still reacted to changes in water vapor levels in the sampling air.

Atmospheric
Measurement
Techniques
Discussions

2.3.2 Cavity pressure monitoring with spectroscopic methods

Cavity pressure of Picarro analyzers affects the width of absorption lines used to measure target gas mole fractions, and the optical phase length (physical path length times refractive index) of the measurement cavity. Both quantities were used to monitor cavity pressure.

5 The CO_2 absorption line is not a good choice for this experiment, because it has a strong line broadening effect with water vapor (Chen et al., 2010). The CH_4 absorption feature is also a poor choice, because it is not a clean, isolated line. Instead, a CRDS analyzer measuring O_2, $\delta^{18}O$ and H_2O (G2207-i, Picarro, Inc., Santa Clara), which works with an O_2 absorption line at 7878.805547 cm^{-1} (John Hoffnagle, personal communication), was used. The active cavity pressure stabilization system of this analyzer is identical to that of Picarro GHG analyzers with the exception that it operates at 339.97 hPa (255 Torr) rather
10 than 186.65 hPa. Therefore, we expect the dependence of cavity pressure on water vapor of this analyzer to be of similar scale and form as for GHG analyzers.

Both O_2 line width and optical phase length are also influenced directly by water vapor: pressure broadening of absorption line widths has been shown in a variety of systems to be dependent upon the background gas matrix, and in particular on water vapor (Chen et al., 2010; Johnson and Rella, 2017; Nara et al., 2012). We therefore expect a linear dependence of the
15 O_2 line width on water vapor mole fraction. Similarly, the index of refraction of air also depends on the gas matrix (Chen et al., 2016), leading to a linear dependence of the optical phase length on water vapor mole fraction. Hence, we attribute non-linear dependencies of O_2 line width and optical phase length on water vapor to changes in cavity pressure.

2.4 Experiments for inferring sensitivities to varying cavity pressure

To determine how readings of the external pressure sensor, CO_2, CH_4, and H_2O (Picarros #1–#5), and O_2 line width and
20 optical phase length (Picarro #6) react to changes in internal cavity pressure, calibration experiments were performed. For these experiments, air from a gas tank was measured with the Picarro analyzer. Initial equilibration periods of readings from the external pressure sensor, CO_2 and CH_4 (Picarros #1–#5), and of O_2 line width and optical phase length (Picarro #6) were discarded. Then, cavity pressure was varied using Picarro Inc. software. Cavity pressure levels were chosen so that their range spanned between dry and humid air in water correction experiments was covered, and probed for several minutes each.
25 Most sensitivity experiments were performed with dry air. With Picarro #3, an additional sensitivity experiment was performed at a water vapor level of 3 % H_2O.

2.5 Water correction experiments with external pressure monitoring

Experiments with stable water vapor levels

During stable water vapor level experiments with external pressure monitoring, water vapor levels were probed between 15
30 and 150 minutes (median about 40 minutes) depending on the stability of the external pressure measurement and trace gas readings. External pressure readings drifted on a timescale of several hours. Therefore, they were calibrated by probing dry

air before and after each measurement in humid air. For further analysis, average readings from the Picarro GHG analyzer and the external pressure sensor of the last 10 minutes of each probing interval were used (15 minutes during the experiment with Picarro #3, five minutes for some low water vapor levels with Picarro #1). The order of water vapor levels was altered between experiments, including high–low–high patterns and random alternations. Varying water levels monotonically

5   throughout an experiment was avoided to ensure that the influence of various potential error sources was not systematic (Sect. S3).
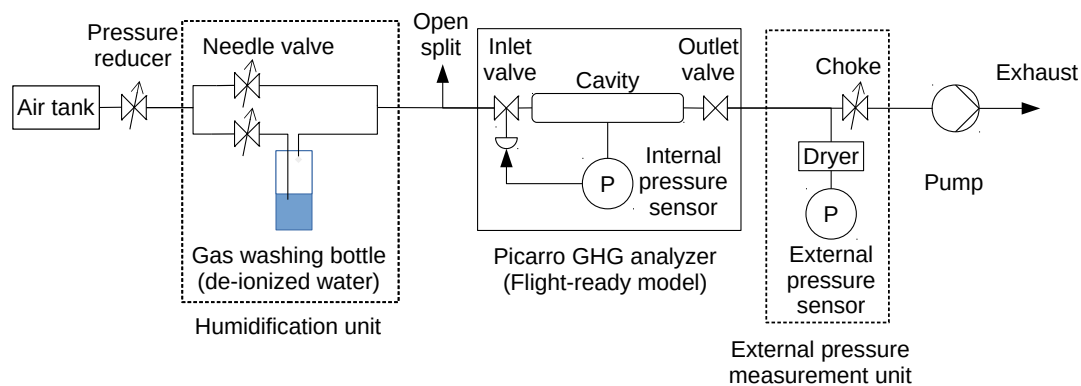
Fig. 1: Experimental setup for water correction experiments with stable water vapor levels and external pressure monitoring. For some experiments, modified setups were used depending on the type of Picarro analyzer and goal of the experiment (see text for

10   details).

Droplet experiments

Droplet experiments with external pressure monitoring were performed with Picarro #1 using the setup shown in Fig. 2. For each droplet experiment, the tee piece was opened, a droplet of deionized water (~ 1 ml) was injected using a syringe, and

15   the tee piece was closed. Gradual evaporation of this water droplet then caused a gradient over time from high to low water vapor levels in the sample air.

Atmospheric
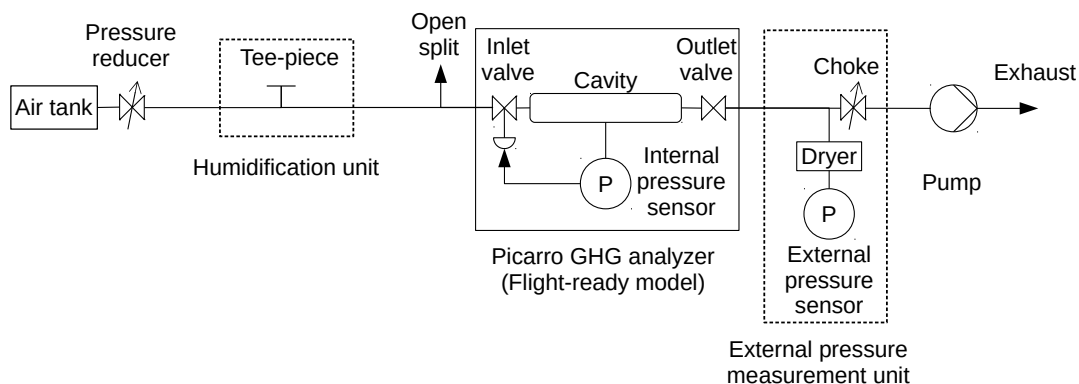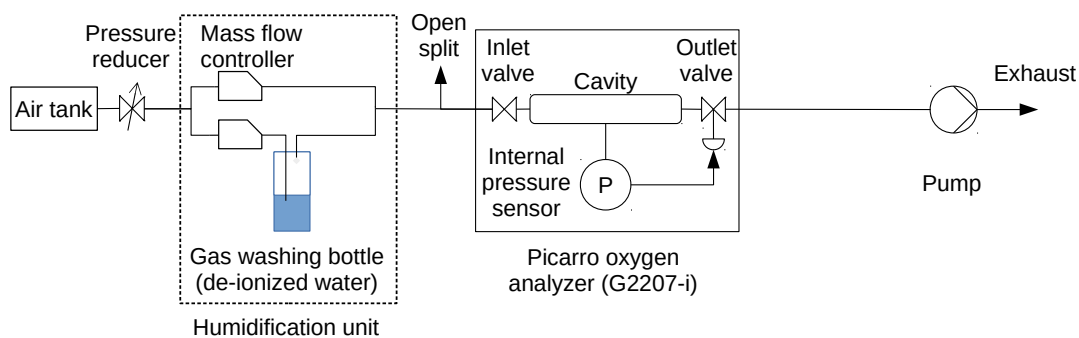Measurement
Techniques
Open Access
Discussions
EGU

Fig. 2: Experimental setup for water correction experiments with humidification via water droplets and external pressure monitoring. Here, the setup for a flight-ready analyzer is shown.

5   2.6   **Experiments for spectroscopic cavity pressure measurements**

For spectroscopic cavity pressure measurements, water vapor was ramped up and down with a period of about 240 minutes for several cycles using the setup depicted in Fig. 3. The water vapor range for the first five cycles was 0–0.2 % H_2O. For another six cycles, the range was extended to 0.8 % H_2O.

10   **Fig. 3: Experimental setup for spectroscopic cavity pressure measurements.**

Atmospheric
Measurement
Techniques
Discussions

3   Results

In this section, we first demonstrate the relevance of cavity pressure for CO_2 and CH_4 measurements performed with Picarro GHG analyzers and establish the sensitivities of the independent pressure monitoring methods to changes in cavity pressure (Sect. 3.1). We then present our results on the dependency of cavity pressure on water vapor (Sect. 3.2), and introduce
5   modifications to the standard water correction model for CO_2 and CH_4 that account for this sensitivity (Sect. 3.3). Finally, we examine the performance of standard and modified water correction models in water correction experiments with stable water vapor levels (Sect. 3.4) and droplet experiments (Sect. 3.5).

3.1   Sensitivity experiments

In the sensitivity tests with Picarro GHG analyzers, readings from the external pressure sensor, as well as of CO_2 and CH_4 all
10   varied linearly with cavity pressure, demonstrating that biases in cavity pressure directly affect mole fraction readings. Similar slopes were observed for all analyzers (Table 2). A sensitivity of water vapor readings to cavity pressure could not be detected. The slopes obtained in the experiment with humid air (3 % H_2O) were very similar to those obtained in dry air with this analyzer (CO_2: +5 %, CH_4: -2 %, external pressure readings: -1 %;). Hence, all slopes were treated as independent of the water vapor mole fraction.
15   In the sensitivity tests with the O_2 analyzer, both the O_2 line width and the optical phase length of the cavity varied linearly with cavity pressure, with the slopes shown in Table 2.

Table 2: Sensitivities of readings of Picarro GHG analyzers and independent pressure measurements to variations of internal cavity pressure p. For the quantities pertaining to GHG analyzers, averages and standard deviations of all sensitivity experiments
20   **with Picarros #1–#3 are reported, while for the quantities pertaining to the O_2 analyzer, mean and standard error of the fit of the single experiment are given.**

Quantity	Analyzer	Sensitivity to cavity pressure
External pressure measurement $\left(\frac{\partial p_{ext}}{\partial p}\right)$	#1–#3	(0.95 ± 0.04) hPa hPa^{-1}
$CO_2 \left(\frac{\partial CO_2}{\partial p}/CO_2^{dry}\right)$	#1–#3	$(9.2 \pm 0.3) \times 10^{-4}$ hPa^{-1}
$CH_4 \left(\frac{\partial CH_4}{\partial p}/CH_4^{dry}\right)$	#1–#3	$(3.22 \pm 0.05) \times 10^{-3}$ hPa^{-1}
O_2 line width	#6	$(4.05 \pm 0.05) \times 10^{-3}$ hPa^{-1}
Optical phase length	#6	(163 ± 3) nm hPa^{-1}

### 3.2   Dependency of cavity pressure on water vapor

3.2.1   Results from external pressure sensor (stable water vapor levels)

25   **Experimental results**

Cavity pressure was monitored with the external sensor during experiments with stable water vapor levels with three different Picarro GHG analyzers. Readings of the internally mounted cavity pressure sensors were, owing to the active pressure stabilization system of the analyzers, stable at 186.65 hPa with standard deviations of 0.02 hPa or less. Cavity pressure was estimated based on external pressure sensor readings and their sensitivity to cavity pressure variations (Sect.

5   3.1). Cavity pressure estimated in this way varied systematically with the water vapor mole fraction, displaying a uniform pattern for all three analyzers (Fig. 4): cavity pressure decreased when the water vapor level increased, and the gradient of the variation was larger below about 0.2 % H_2O, which created a bend in the dependency of cavity pressure on water vapor (henceforth called "pressure bend").
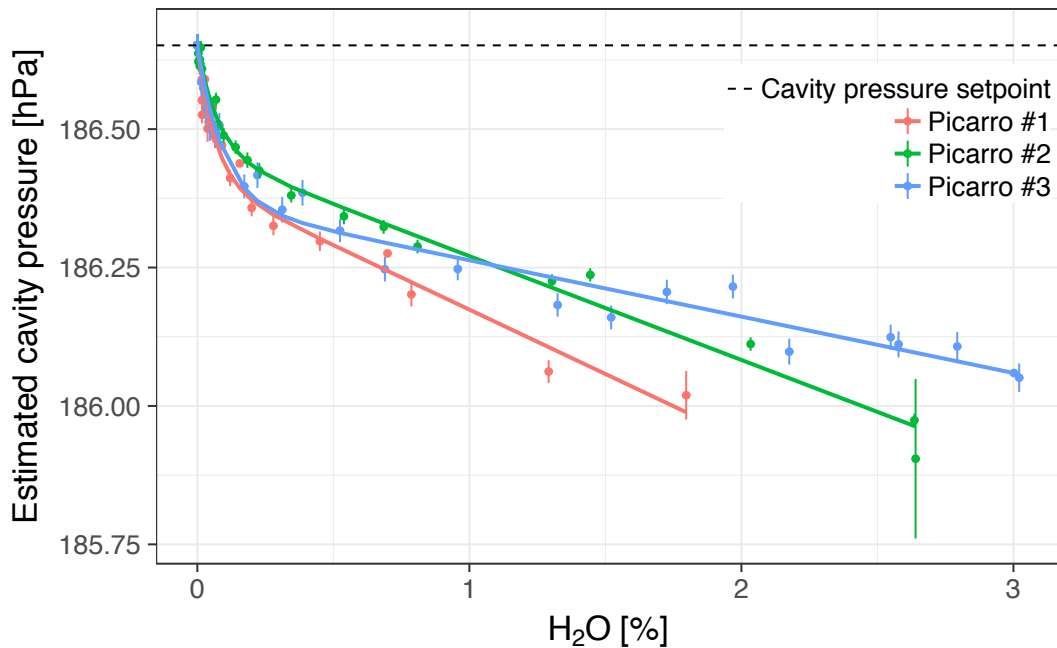
10   **Fig. 4: Cavity pressure estimated based on external pressure sensor readings in experiments with stable water vapor levels and fits of the empirical cavity pressure model Eq. (4) to the data. Error bars: lower bound of uncertainty; see Sect. S1.2.**

Empirical description

Based on these results, we formulated an empirical description of cavity pressure dependency on water vapor:

$$p_{est}(h) = p_0 + s \cdot h + d_p \cdot \left(e^{-\frac{h}{h_p}} - 1 \right)$$

(4)

9

In this equation, p_{est} is the estimated cavity pressure, h is the water vapor mole fraction, p_0 is the cavity pressure in dry air (186.65 hPa for Picarro GHG analyzers), h_p is the position of the pressure bend, s is the slope for $h \gg h_p$, and d_p describes the magnitude of the pressure bend.

The empirical cavity pressure model Eq. (4) was fitted to the data of each analyzer. The coefficient of determination was

5   larger than 0.98 for all experiments, indicating good fits. Estimated coefficients varied between analyzers (Table 3).

Table 3: Coefficients of the empirical cavity pressure model Eq. (4) for data from experiments with stable water vapor levels and external pressure monitoring (estimate and standard error). The last line shows averages and standard deviations of the individual estimates.

Analyzer	s [hPa (% H_2O)$^{-1}$]	h_p [% H_2O]	d_p [hPa]
#1	-0.131 ± 0.009	0.066 ± 0.009	0.245 ± 0.016
#2	-0.106 ± 0.003	0.076 ± 0.009	0.193 ± 0.009
#3	-0.057 ± 0.004	0.095 ± 0.011	0.286 ± 0.012
Average	-0.10 ± 0.04	0.079 ± 0.014	0.24 ± 0.05

10   ### 3.2.2   Results from external pressure sensor during droplet experiments

Cavity pressure estimated based on external pressure sensor readings varied strongly between droplet experiments and was consistently lower than during the stable water vapor level experiment with this analyzer (Fig. 5, top panel). The largest variations occurred below 1 % H_2O. In this domain, the droplets dried up quickly, which caused very fast decreases of the water vapor mole fraction from about 0.5–1 % to 0 % H_2O (Fig. 5, bottom panel).
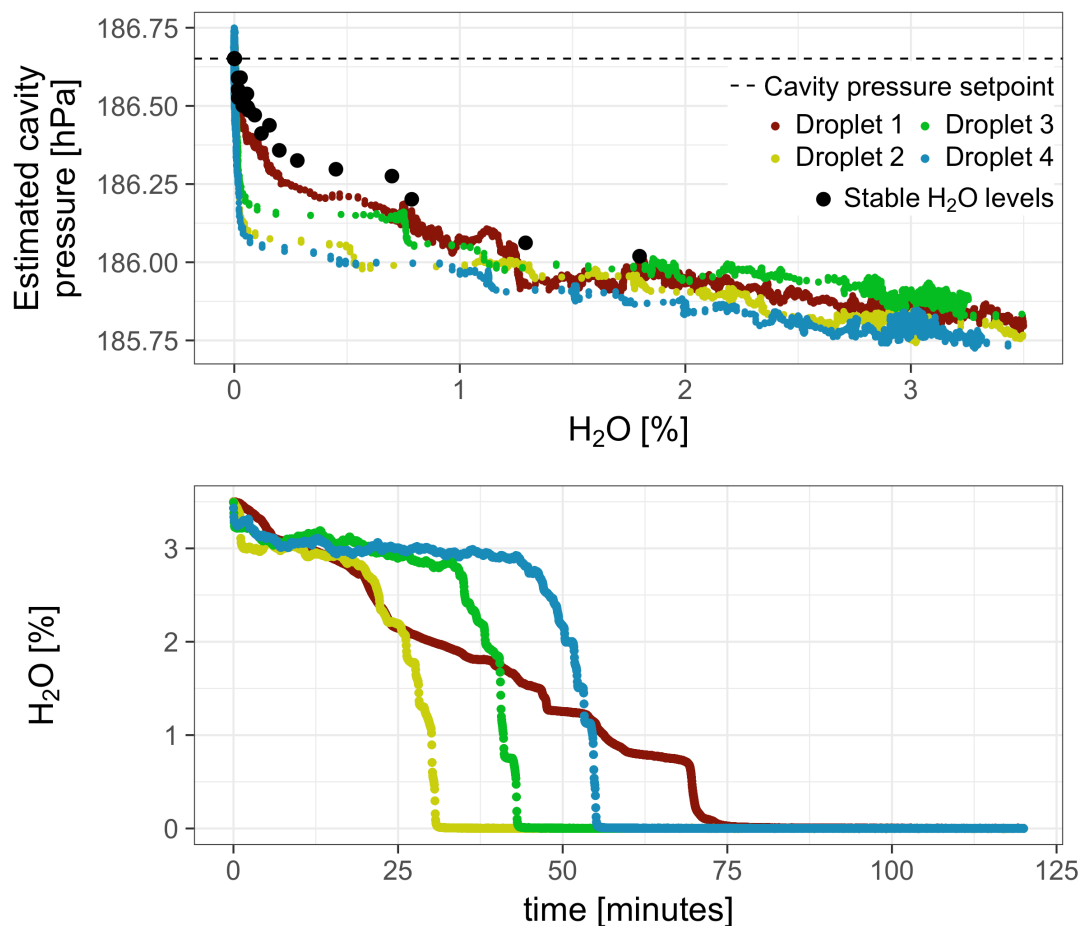
Fig. 5: Top: Cavity pressure during droplet experiments with Picarro #1 estimated based on data from the external pressure sensor. For reference, the results from the experiment with stable water vapor levels from this analyzer are plotted as well (same as in Fig. 4). Bottom: Temporal progression of water vapor mole fraction during the droplet experiments after the drop below 3.5 % H_2O.

3.2.3   Results from spectroscopic cavity pressure measurements

The O_2 line width measurements were stable throughout the experiment (not shown). To reduce their noise, they were averaged over periods of 100 seconds. By contrast, the optical phase length of the cavity drifted over the course of the

11

Atmospheric
Measurement
Techniques
Discussions

experiment (explained in Sect. S2). Therefore, the averaged data based on the phase length were binned for further analysis, separately for the cycles between 0 and 0.2 % H_2O and those between 0 and 0.8 % H_2O.

At water vapor mole fractions above 0.2 % H_2O, cavity pressure estimates based on optical phase length and O_2 line width both showed linear dependencies on water vapor, potentially with a small nonlinear component in the O_2 line width data

5 (Fig. 6). The linear dependencies can be ignored here, as they are compounded by effects other than cavity pressure changes (Sect. 2.3.2). Below about 0.2 % H_2O, both estimates exhibited the pressure bend that was also observed with the external pressure sensor. Fitting the empirical cavity pressure model Eq. (4) yielded coefficients for pressure bend position and magnitude very similar to those derived from data of the external pressure sensor (Table 4) and coefficients of determination larger than 0.98, which indicates good fits.
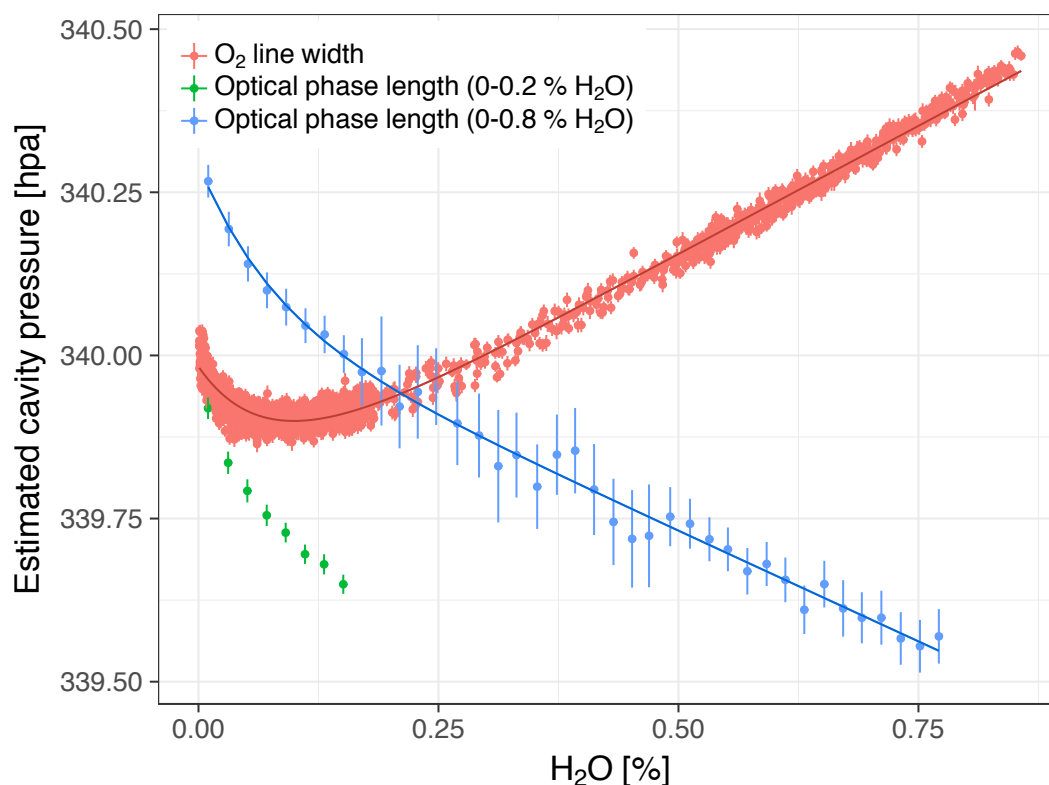
10

Fig. 6: Cavity pressure estimated based on spectroscopic pressure measurements with Picarro #6 and fits of Eq. (4). Error bars of O_2 line widths and optical phase lengths are the standard errors of averaging and binning, respectively. Since the cycles up to 0.2 % H_2O did not extend into the linear domain, the model was not fitted to the optical phase length data of these cycles.

Atmospheric
Measurement
Techniques
Discussions

Table 4: Coefficients for the empirical cavity pressure model Eq. (4) based on spectroscopic methods (estimates and standard errors). The last line shows averages and, as uncertainty, half the spreads of the individual estimates. The average of the slopes is not given because the slopes are caused by different physical processes.

Method	s [hPa (% H$_2$O)$^{-1}$]	h_p [% H$_2$O]	d_p [hPa]
O$_2$ line width	0.443 ± 0.002	0.076 ± 0.002	0.221 ± 0.002
Optical phase length	-0.38 ± 0.02	0.078 ± 0.019	0.222 ± 0.024
Average	-	0.0767 ± 0.0008	0.2216 ± 0.0006

5

3.3 Modification of standard water correction model to account for cavity pressure sensitivity to water vapor

Based on the results from sensitivity experiments and independent cavity pressure measurements, the standard water correction model Eq. (3) was modified to account for cavity pressure sensitivity to water vapor. First, the impact of measured deviations of cavity pressure from its nominal value ($\Delta p = p - p_0$) was subtracted from the wet air mole fractions. Then, the

10 standard water correction model was applied to the modified wet air mole fractions:

$$c_{dry}^{pressure-correction} = \frac{c_{wet}(h) - \frac{\partial c}{\partial p} \cdot \Delta p}{f_c^{para}(h)} \qquad (5)$$

Here, $\frac{\partial c}{\partial p}$ is the sensitivity of the trace gas to cavity pressure changes. Henceforth, we call this the "pressure-correction" model.

The pressure-correction model requires independent measurements of cavity pressure. To eliminate the need for such measurements, the model was reformulated based on the empirical pressure correction model by substituting Δp in Eq. (5)

15 with ($p_{est} - p_0$) from Eq. (4) and rearranging the terms yields

$$c_{dry}^{expanded} = \frac{c_{wet}(h)}{f_c^{exp}(h)} \qquad (6)$$

with an "expanded" water correction function $f_c^{exp}(h)$:

$$f_c^{exp}(h) = \underbrace{1 + a_c \cdot h + b_c \cdot h^2}_{f_c^{para}(h)} + d_c \cdot \left(e^{-\frac{h}{h_p}} - 1 \right) \qquad (7)$$

Here, h_p is the pressure bend position from Eq. (4), and $d_c = d_p \cdot \frac{\partial c}{\partial p}$. Possible sensitivity of $\frac{\partial c}{\partial p}$ to water vapor, which was not detected in sensitivity experiments (Sect. 3.1), was neglected here. Coefficients for this model can be estimated from trace gas data, i.e. independent cavity pressure measurements are not needed.

Atmospheric
Measurement
Techniques
Open Access
EGU
Discussions

3.4 Water corrections based on experiments with stable water vapor levels

3.4.1 Experiment with external pressure measurement

In this section, we show biases of the standard water correction model and link them to the cavity pressure sensitivity to water vapor. For this purpose, we collected data for both cavity pressure and the target gases CO_2 and CH_4 in one stable

5   water vapor level experiment (with Picarro #3). We compare dry air mole fractions based on the standard, pressure-correction and expanded water correction models (Eq. (3), (5) and (6), respectively).
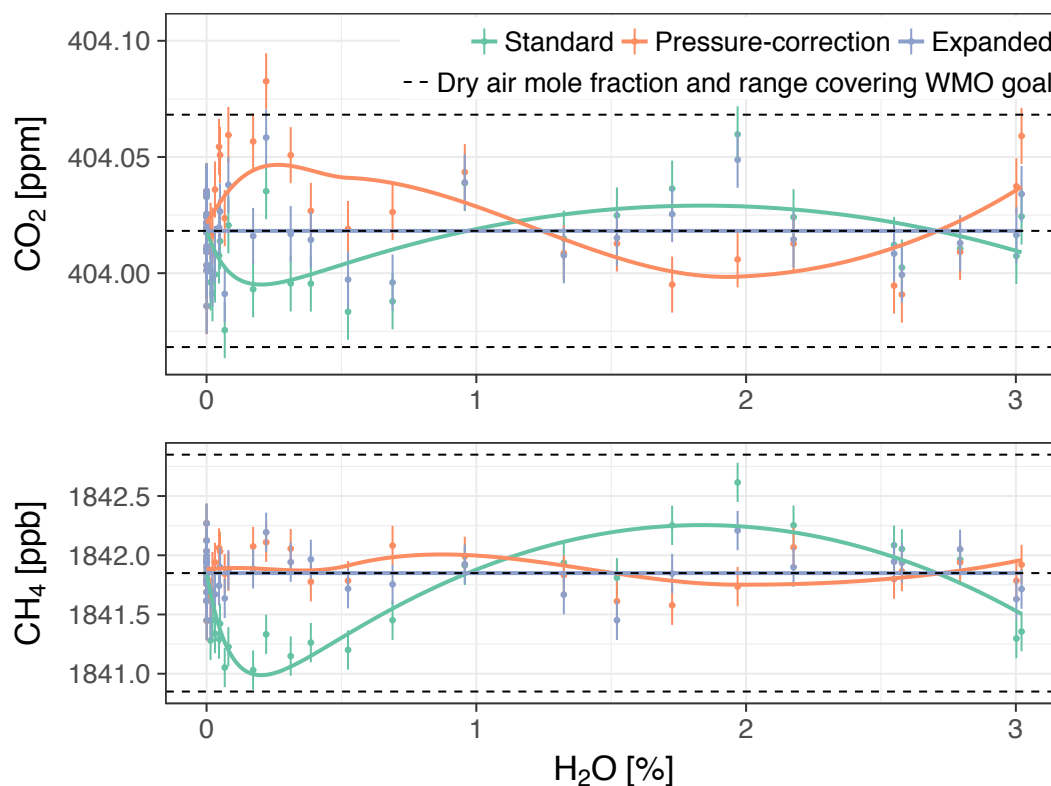

Fig. 7: Dry air mole fractions from the experiment with Picarro #3 based on the three water correction models. Error bars: one standard deviation of the trace gas mole fractions measured in dry air. The solid lines are the biases of the models assuming the
10   **expanded model was unbiased (smoothed for the pressure-correction model), offset by the mole fractions measured in dry air.**

Dry air mole fractions of CH_4 calculated using the standard water correction model had a water-dependent structure (Fig. 7, bottom panel), with sustained negative biases at water vapor levels below 1 % H_2O as the most prominent feature. This

14

structure was eliminated by the pressure-correction and the expanded model, so that the dry air mole fractions based on these models varied less (Table 5). The largest difference between standard and expanded water correction model occurred at 0.2 % H_2O (Table 6). Differences between pressure-correction and standard model were small (Fig. 7, bottom panel).

5   For CO_2, dry air mole fractions based on the standard model had a similar structure as the CH_4 mole fractions, but the differences to the expanded water correction model, which performed best, were much smaller than for CH_4 in terms of the overall variability (Table 5) and compared to the WMO goals in the northern hemisphere (Fig. 7, top panel, Table 6). The pressure-correction model showed a comparatively poor performance, dominated by a small bias similar to the one present in the results of the standard model but with opposite sign (Fig. 7, top panel).

10   **Table 5: Standard deviations of dry air mole fractions based on different water correction models from the experiment with Picarro #3.**

| Model	St. dev. CO_2	St. dev. CH_4
Standard	0.017 ppm	0.35 ppb
Pressure-correction	0.019 ppm	0.16 ppb
Expanded	0.014 ppm	0.18 ppb

Table 6: Maximum differences between dry air mole fractions based on standard and expanded water correction model from the experiment with Picarro #3. The largest differences are also given as percentages of the mole fractions measured in dry air.

	CO_2	CH_4	Position
Negative	0.023 ppm / 0.006 %	0.86 ppb / 0.047 %	0.2 % H_2O
Positive	0.011 ppm	0.41 ppb	1.7 % H_2O
Range	0.034 ppm	1.30 ppb	

15

3.4.2   Variability between experiments with the same analyzer

With Picarro #5, one gas washing bottle experiment was performed in each 2015 and 2017, without external cavity pressure monitoring. In the 2015 experiment, the number of data points was insufficient to fully constrain both h_p and d_c in the expanded water correction model. Since the (uncertain) estimate of h_p based on CH_4 was close to the mean of h_p from the

20   three experiments with external cavity pressure monitoring ($h_p^{mean} = (0.079 \pm 0.014)$ % H_2O), h_p was set to h_p^{mean} for this experiment (using the coefficients from the 2017 experiment induced biases in water-corrected CH_4 mole fractions). For the 2017 experiment, the estimate of h_p based on CH_4 data was used also for CO_2, because its estimate based on CO_2 data was highly uncertain.

Atmospheric
Measurement
Techniques
Discussions
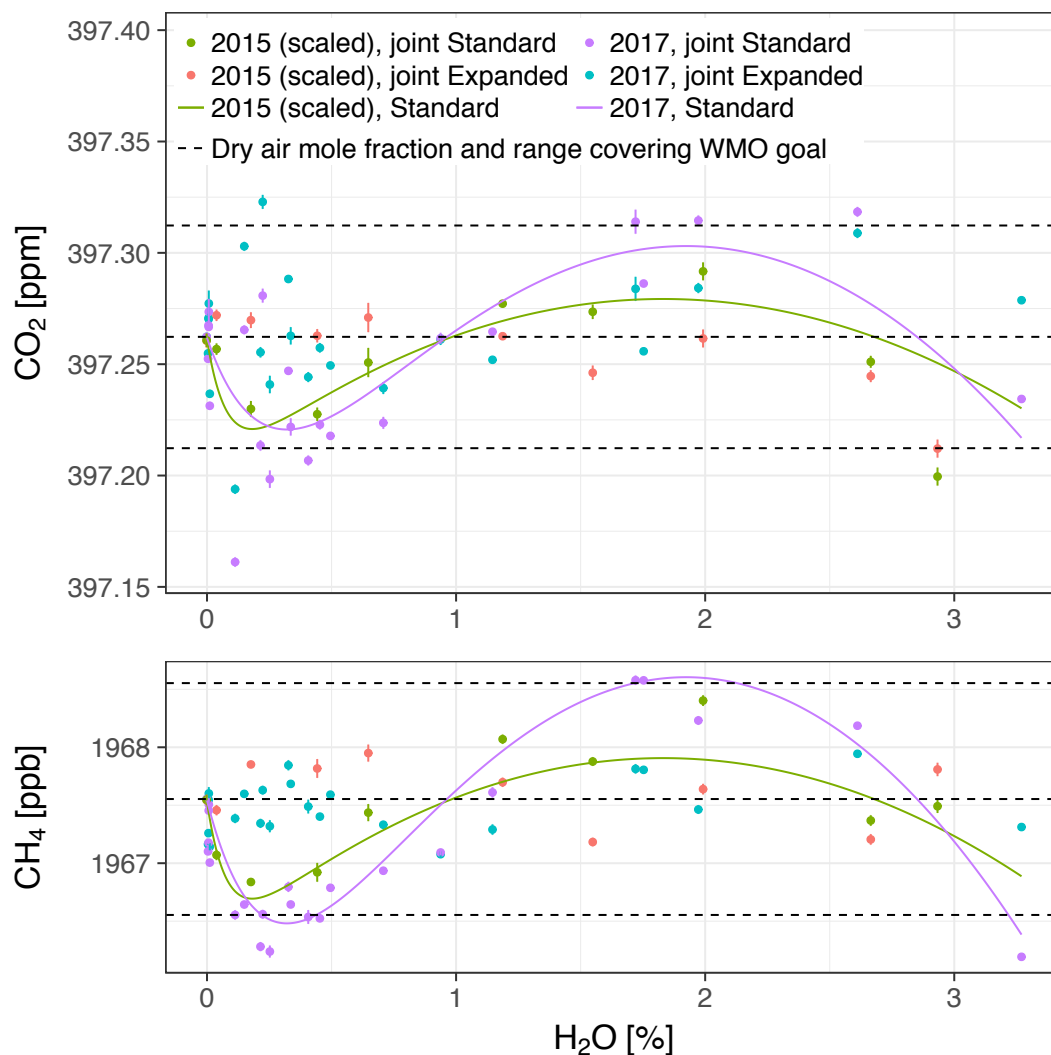
Fig. 8: Water-corrected dry air mole fractions from the two experiments with Picarro #5. The data from the 2015 experiment have been scaled up to match the mole fractions measured in dry air in the 2017 experiment. The points are based on model fits to data from both experiments jointly (error bars: lower bounds of uncertainty; see Sect. S3), while the solid lines show differences between standard and expanded water correction model fitted to data from the 2015 and the 2017 experiments individually, offset by the mole fractions measured in dry air in the 2017 experiment.

16

Atmospheric
Measurement
Techniques
Discussions

For both experiments, dry air mole fractions of CO_2 and CH_4 obtained using the standard water correction model had negative biases around the pressure bend position and at the highest sampled water vapor mole fractions (3 % H_2O), and a positive bias in between (lines in Fig. 8, Table 7). The biases were eliminated by the expanded model (Table 7). The magnitudes of the biases of water-corrected CO_2 mole fractions were consistent with those of CH_4. In the 2015 experiment,

5   the largest bias occurred around the pressure bend position, while in the 2017 experiment, the largest positive biases, which occurred at 1.9 % H_2O, and the negative biases at the highest sampled water vapor mole fractions were on par with those at the pressure bend position (Table 7). Residuals were much larger than the estimated lower bounds of the uncertainty (error bars in Fig. 8), owing to the fact that not all uncertainties could be quantified (Sect. S3).

10   **Table 7: Comparison of water corrections of the two experiments with Picarro #5. The bias estimates of the standard model are based on the assumption that the results of the expanded model were unbiased.**

	CO_2		CH_4	
	2015 experiment	2017 experiment	2015 experiment	2017 experiment
Coefficients (individual experiments)				
h_p	See CH_4	See CH_4	(0.079 ± 0.014) % H_2O (from Table 3)	(0.26 ± 0.06) % H_2O
d_c	$(1.6 \pm 0.3) \times 10^{-4}$	$(3.0 \pm 0.6) \times 10^{-4}$	$(6.6 \pm 1.1) \times 10^{-4}$	$(1.7 \pm 0.1) \times 10^{-3}$
Coefficients (joint correction with data from both experiments)				
h_p	See CH_4		(0.16 ± 0.04) % H_2O	
d_c	$(2.3 \pm 0.4) \times 10^{-4}$		$(1.19 \pm 0.08) \times 10^{-3}$	
Standard deviations (individual experiments and joint correction)				
Standard model	0.02 ppm	0.04 ppm	0.39 ppb	0.7 ppb
Expanded model	0.01 ppm	0.02 ppm	0.17 ppb	0.2 ppb
Expanded model (joint correction)	0.016 ppm	0.027 ppm	0.24 ppb	0.23 ppb
Maximum biases of standard model (individual experiments)				
Negative, position (< 1 % H_2O)	0.037 ppm/0.0104 %, 0.18 % H_2O	0.041 ppm/0.0105 %, 0.32 % H_2O	0.78 ppb/0.0437 %, 0.18 % H_2O	1.07 ppb/0.0545 %, 0.32 % H_2O
Positive, position	0.015 ppm, 1.8 % H_2O	0.043 ppm, 1.9 % H_2O	0.32 ppb, 1.8 % H_2O	1.10 ppb, 1.9 % H_2O
Maximum differences by swapping coefficients of expanded model between individual experiments				
< 1 % H_2O	0.02 ppm/0.049 %		0.6 ppb/0.030 %	
> 3 % H_2O	0.07 ppm/0.018 %		0.4 ppb 0.022 %	

The water correction coefficients obtained from the two experiments had significant differences (Table 7). To assess the impact of these differences on water-corrected dry air mole fractions, two analyses were performed. First, the coefficients of either experiment were applied to the other one. This resulted in differences around the pressure bend positions, but they were smaller than the differences between standard and expanded water correction model. In addition, CO_2 differed at the largest water vapor mole fraction sampled (Fig. 8, top panel, Table 7). For a second assessment of differences between the two experiments, the 2015 data was scaled up to the mole fractions measured in dry air in the 2017 experiment and expanded model was fitted to all data to obtain joint water corrections (points in Fig. 8). Standard deviations of the water-corrected dry air mole fractions based on the joint correction were between those based on the individual standard and expanded models (Table 7).

3.4.3   A case without bias of the standard water correction model

With Picarro #4, a gas washing bottle experiment without independent cavity pressure monitoring was performed. Dry air mole fractions obtained with the standard water correction model did not exhibit the systematic biases observed in Picarros #3 and #5 (Fig. 9) and had standard deviations of 0.016 ppm CO_2 and 0.21 ppb CH_4. This is better than the performance of the standard model in the experiments with the other analyzers, and for CH_4 close to the performances of the expanded model. Applying the expanded model to these data yielded insignificantly small pressure bend magnitudes d_c and thus very similar dry air mole fractions without improvement of the variability (not shown). Residuals were much larger than the estimated lower bounds of the uncertainty (error bars in Fig. 9), owing to the fact that not all uncertainties could be quantified (Sect. S3).
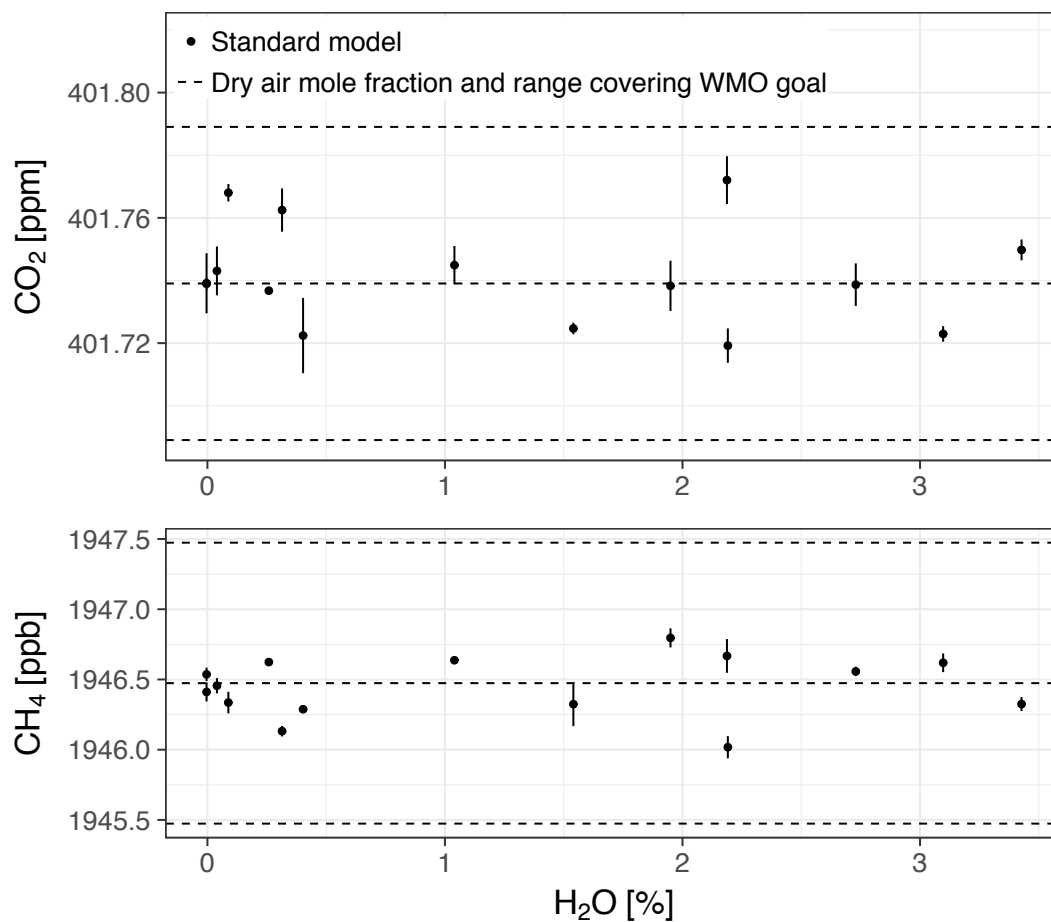
Fig. 9: Dry air mole fractions of CO_2 and CH_4 for a gas washing bottle experiment with Picarro #4 based on the standard water correction model. Error bars: lower bound of uncertainty; see Sect. S3.
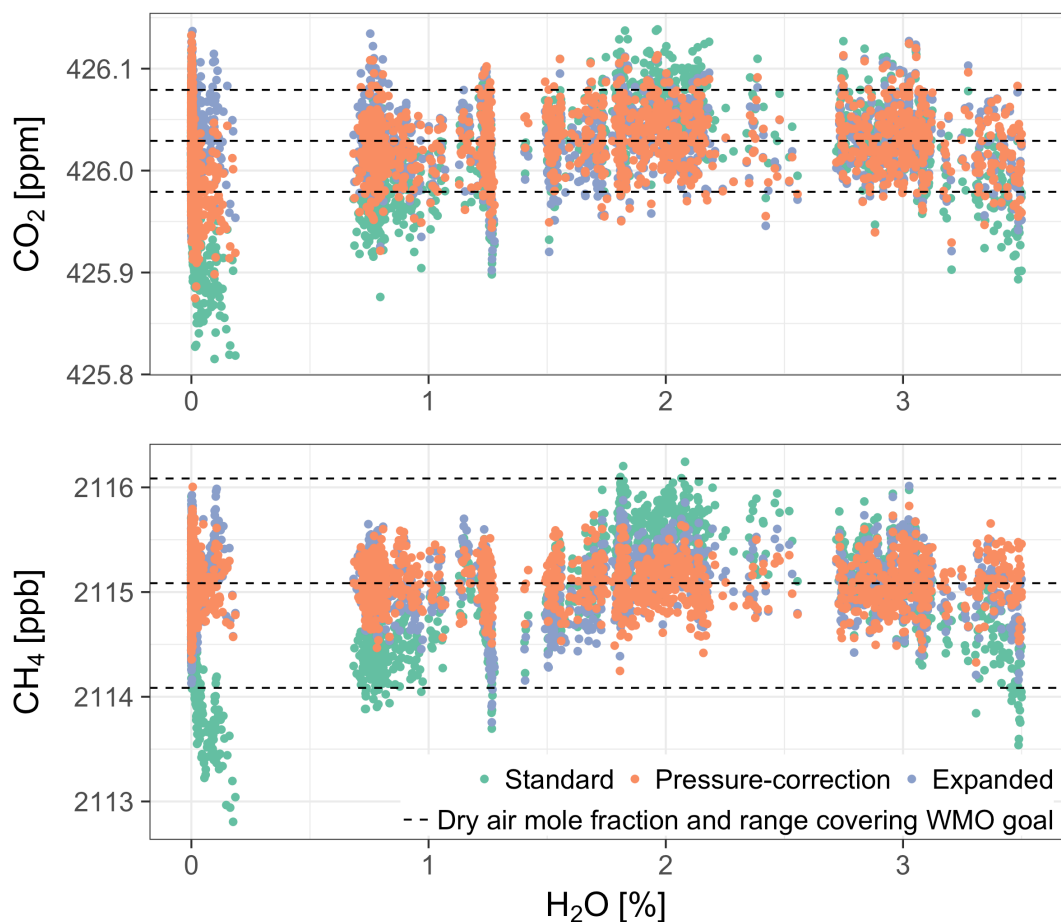
5   3.5   **Water corrections based on droplet experiments**

The water correction models were fitted to data from droplet experiments where the water vapor mole fraction, selected for data below 3.5 % H_2O and where the difference between subsequent H_2O measurements was smaller than 0.005 % H_2O. The former filter ensured compatibility with the gas washing bottle experiments, while the latter was an empirical filter to

19

Atmospheric
Measurement
Techniques
Discussions

exclude the fastest water vapor variations, which resulted in large variations of CO_2 and CH_4 readings, while leaving enough data for fitting.

Dry air mole fractions obtained with the standard water correction model had the typical bias structure that was also observed during gas washing bottle experiments (compare Fig. 10 with Fig. 7 and Fig. 8). Both the pressure-correction and the expanded model reduced or eliminated the biases induced by the standard model, with better performance of the pressure-correction model (Table 8). While the CH_4 bias at low water vapor mole fractions was eliminated by the pressure-correction model, the bias of CO_2 was only reduced.

20

Atmospheric
Measurement
Techniques
Discussions

Fig. 10: Dry air mole fractions from droplet experiment 1 with Picarro #1 based on the three water correction models. Droplet 1 is shown because it yielded the most data points after applying the filters described in the text.

Table 8: Average standard deviations of dry air mole fractions from all droplet experiments with Picarro #1 based on the three water correction models.

Model	St. dev. CO_2	St. dev. CH_4
Standard	0.042 ppm	0.42 ppb
Pressure-correction	0.036 ppm	0.26 ppb
Expanded	0.039 ppm	0.35 ppb

5

During the fast decreases of water vapor mole fractions from about 0.5–1 % to 0 % H_2O (Sect. 3.2.2), differences between wet air mole fractions between droplet experiments were large. The differences were quantified based on fitting the water correction functions of all models to wet air mole fractions from the individual droplets. The expanded function captured the large differences, which were up to 0.17 ppm CO_2 and 6.0 ppb CH_4 (Fig. 11). By contrast, differences between fits of the

10 parabolic water correction function to wet air mole fractions (standard model), as well as to pressure-corrected wet air mole fractions (pressure-correction model), were much smaller, i.e. 0.04 ppm CO_2 and 0.8 ppb CH_4 (not shown).
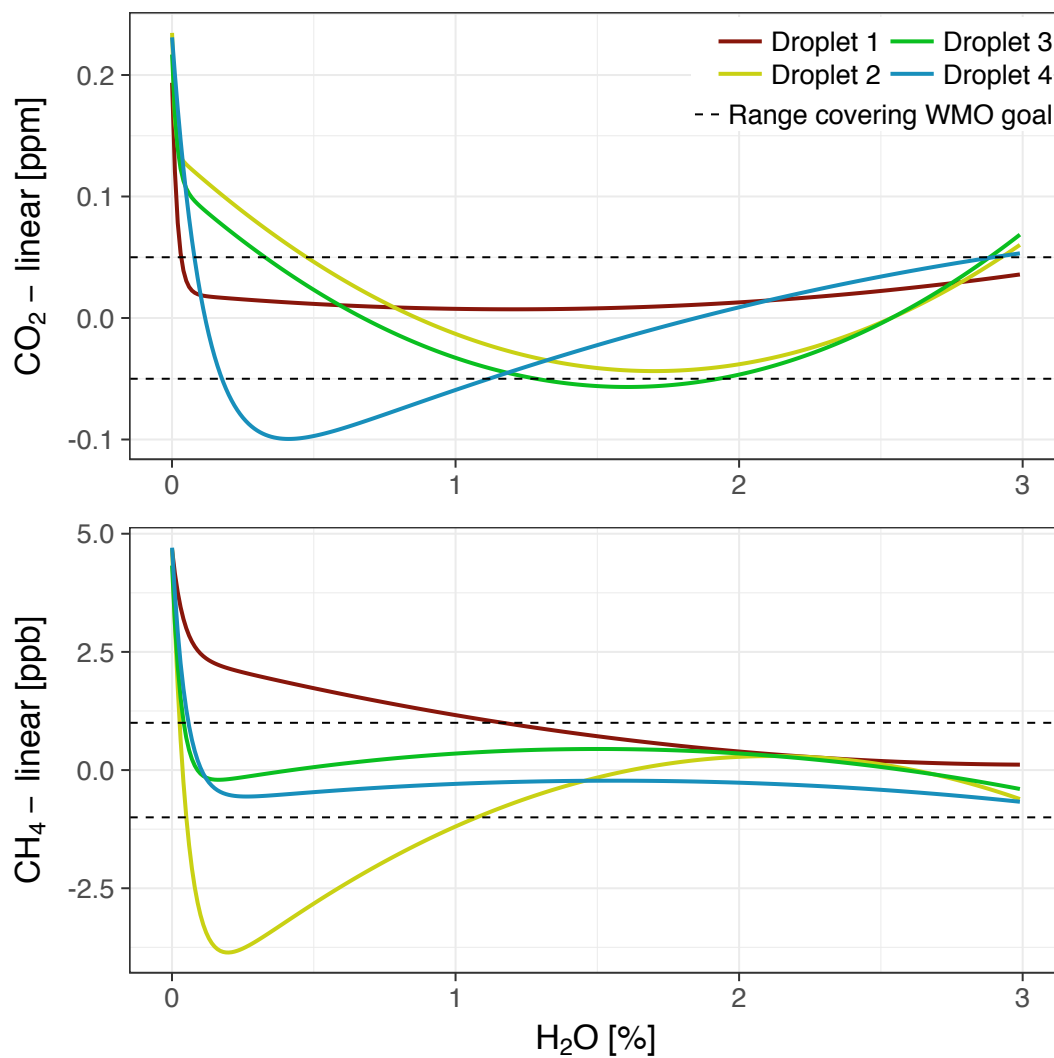
Fig. 11: Expanded water correction model fitted to data from four droplet experiments with Picarro #1. To emphasize the large differences, a common linear component has been subtracted.

Atmospheric
Measurement
Techniques
Discussions

4   Discussion

4.1   Findings from sensitivity experiments

Sensitivity experiments revealed sensitivities of CO_2 and CH_4 readings of Picarro GHG analyzers to cavity pressure. This demonstrates that trace gas readings are affected by systematic biases of cavity pressure.

5   Furthermore, these sensitivity experiments established the ability of our independent cavity pressure monitoring methods to detect cavity pressure changes. As a caveat, the sensitivity experiments did not rule out water-dependent biases of the independent cavity pressure monitoring methods. In particular, although readings from the external pressure sensor showed the same sensitivity to cavity pressure in dry and humid air, there may have been a water-dependent bias in these readings (more details in Sect. S1). Furthermore, we did not check whether the sensitivities of O_2 line width and optical phase length
10   to cavity pressure depended on water vapor. However, the key result of our experiments, the pressure bend, was broadly consistent between data from the external pressure sensor, both spectroscopic cavity pressure estimates, and CH_4 data. Given that all of these quantities were estimated based on different, unrelated methods, it is unlikely that our independent cavity pressure monitoring methods had systematic, water-dependent biases that affected our conclusions.

4.2   Cavity pressure of Picarro analyzers is sensitive to water vapor

15   Results from all independent cavity pressure measurements demonstrate that cavity pressure of Picarro analyzers is sensitive to the water vapor content of the sample air. We described the sensitivity empirically based on the results of experiments with stable water vapor levels and external cavity pressure monitoring with Eq. (4).

Results from either humidification method indicate that cavity pressure takes time to adjust to new water vapor levels. To investigate whether cavity pressure equilibration affected the conclusions drawn from water correction experiments with
20   stable water vapor levels, we inspected long (5–12 hours) dry air measurements for evidence of cavity pressure equilibration longer than our typical probing time of humid air (40 minutes) and found only small variations (Sect. S1.1). We did not check for long equilibration after switching from dry to humid air. However, both in gas washing bottle and in droplet experiments, there was no indication that cavity pressure equilibrated more slowly with increasing than with decreasing water vapor mole fraction. Therefore, it is unlikely that cavity pressure equilibration affected the conclusions drawn from the
25   experiments with stable water vapor levels.

Results from spectroscopic cavity pressure measurements agreed with the results of the external pressure sensor. Both the estimate based on O_2 line width and the one based on optical phase length exhibited the pressure bend with the same sign, and at a position and magnitude close to the average of the estimates based on the external pressure sensor. We note that we expected the magnitude of the pressure bend to scale with cavity pressure instead, i.e. that it would be larger than estimates
30   based on GHG analyzers by a factor of ≈ 1.8, the ratio of cavity pressures of these instruments. Given the variability of d_p between the three experiments with GHG analyzers, it is not certain whether this was the case.

23

We speculate that the observed sensitivity of internal pressure readings to humidity levels in sampled air is due to adsorption of H_2O molecules on the pressure sensor inside the cavity. The pressure measurement is based on a piezoresistive strain gauge exposed to the pressure media (air in the cavity). The strain gauge is mounted on a thin diaphragm, which is deflected by pressure. The resulting strain causes a change in electrical resistance and creates an output voltage varying with pressure.

5 Water molecules adsorbed on the strain gauge, diaphragm, or adjacent parts of the sensor may change its response to pressure mechanically, and/or may affect the electrical properties of the circuit. However, elucidating the underlying physical effect of the cavity pressure changes is beyond the scope of this paper, and was not investigated further.

Since CO_2 and CH_4 readings react to changes in cavity pressure, the sensitivity of cavity pressure to water vapor affects CO_2 and CH_4 readings in humid air, and an adequate correction method is required to avoid systematic biases in water-corrected

10 dry air mole fractions.

4.3 Cavity pressure sensitivity to water vapor causes biases in CO_2 and CH_4 readings

The standard water correction model caused biases in water-corrected CO_2 and CH_4 mole fractions in experiments with stable water vapor levels and droplet experiments. The shortcoming of the standard water correction model is that it is unable to model the pressure bend. The pressure-correction model, which directly links cavity pressure to trace gas readings,

15 eliminated the biases in CH_4 in all experiments. Although results for CO_2 were mixed (see Sect. 4.6), the performance of the pressure-correction model demonstrates a link between cavity pressure sensitivity to water vapor and trace gas readings of Picarro GHG analyzers in humid air. Biases of the standard model depend on the dry air mole fraction, and in our experiments amounted to up to 50 % of the WMO inter-laboratory compatibility goal for CH_4 and 80 % of the goal for CO_2 in the southern hemisphere (Picarro #5, 2017 experiment).

20 4.4 Correcting for cavity pressure sensitivity to water vapor without independent cavity pressure measurements

We developed the expanded water correction model to allow correction for the sensitivity of cavity pressure to water vapor without independent cavity pressure measurements. The model was based on the parabolic water correction model from the literature and our empirical description of the dependency of cavity pressure on water vapor, which was composed of a linear term and an exponential term describing the pressure bend. We note that O_2 line width data suggest a small curvature of the

25 cavity pressure dependency beyond the pressure bend (Fig. 6), as do data from the external pressure sensor during droplet experiments at water vapor mole fractions larger than those covered by our experiments with stable water vapor levels (Fig. 5, top panel). However, small curvatures can be captured by the parabolic part of all models, implying the expanded model is suitable despite potential shortcomings of the empirical cavity pressure model it was based on.

4.4.1 Experiments with stable water vapor levels

30 In the water correction experiment with stable water vapor levels and external cavity pressure monitoring, the CH_4 results of the expanded model closely matched those of the pressure-correction model (Sect. 3.4). It also fitted the observed CO_2 mole

fractions from this experiment well, but their inconsistency with data from the external pressure sensor puts these CO_2 data into question (Sect. 4.6). More water correction experiments with stable water vapor levels were performed without independent cavity pressure measurement. In these experiments, consistency with cavity pressure could not be checked directly, but comparing the pressure bend magnitudes d_{CO_2} and d_{CH_4}, as well as estimates of h_p based on either trace gas

5 may help spotting inconsistencies. For instance, in the experiments with Picarro #5, d_{CO_2} and d_{CH_4} were broadly consistent (not shown), while in the experiment with Picarro #3, d_{CO_2} was smaller than expected. In conclusion, CO_2 and CH_4 readings can be corrected for the dependency of cavity pressure on water vapor based on experiments with stable water vapor levels using the expanded water correction model, which does not require independent cavity pressure monitoring.

4.4.2 Droplet experiments

10 During droplet experiments, cavity pressure depended on the temporal course of water vapor variation. In particular, water vapor diminished quickly around the pressure bend position, but with a different temporal course in each experiment. Simultaneously, cavity pressure estimated based on the external pressure sensor was too low and inconsistent in this domain. We conclude that the fast water vapor variations did not allow the measurements of the internal cavity pressure sensor to equilibrate, which caused biased CO_2 and CH_4 readings. While the biases were mitigated by the pressure-correction model,

15 the expanded model captured exaggerated and irreproducible pressure bends. Therefore, the droplet method proved unsuitable for correcting cavity pressure-related biases of CO_2 and CH_4 readings without independent cavity pressure monitoring.

4.5 Coefficients of expanded water correction model vary

4.5.1 Variability between experiments with the same analyzer

20 With Picarro #5, two experiments with stable water vapor levels were performed two years apart. Droplet experiments were also performed with this analyzer, but it was shown that they are not suitable to correct for cavity pressure sensitivity to water vapor without independent cavity pressure measurements (Sect. 4.4), and therefore, we restricted our analysis to the experiments with stable water vapor levels. Coefficients of the expanded model differed significantly between these experiments. It is unclear whether the differences were due to limited reproducibility, short-term variations or long-term

25 drifts, and more experiments are required to understand the variability. Variability may also be caused by other mechanisms than the sensitivity of cavity pressure to water vapor, which may explain the differences at water vapor mole fractions far from the pressure bend position between the two experiments. The differences around the pressure bend position between the two experiments were smaller than biases of the standard model. Therefore, dry air mole fractions in this domain based on either set of coefficients were likely more accurate than those based on the standard model despite the variation between the

30 two experiments.

Atmospheric
Measurement
Techniques
Discussions

Open Access

EGU

4.5.2 Differences between analyzers

In total, we performed water correction experiments for CO_2 and CH_4 with three Picarro GHG analyzers. While the position (h_p) and magnitude (d_c) of the pressure bend in CO_2 and CH_4 readings were broadly consistent between Picarros #3 and #5 (with the exception that the effect on CO_2 of Picarro #3 appeared diminished), CO_2 and CH_4 readings from Picarro #4

5   exhibited no detectable pressure bend. The magnitude of the pressure bend of this analyzer may be smaller than that of the others, masked by random fluctuations, or not be present at all. Alternatively, the pressure bend position may have been at a higher water vapor level, so that the standard model could capture the bend. The differences between this analyzer and the others are not explained by estimated uncertainties (Sect. S3). Thus, they remain an open question for future research. The differences imply that custom coefficients for the expanded model should be obtained for each Picarro analyzer.

10   ### 4.6 Challenges for CO_2

In all water correction experiments with independent cavity pressure monitoring, CO_2 data were not fully consistent with independent cavity pressure data. In the water correction experiment with stable water vapor levels and external pressure monitoring (Picarro #3), biases of dry air CO_2 mole fractions obtained using the standard water correction model were much smaller than expected from cavity pressure variations, i.e. the pressure-correction model overcompensated the bias of the

15   standard model. By contrast, biases of dry air mole fractions of CO_2 obtained using the standard model based on data from droplet experiments were reduced by the pressure-correction model, but not fully eliminated. Since CH_4 data were consistent with data from the external pressure sensor (Sect. 4.3), the most likely cause for the mixed CO_2 results is variations of the CO_2 mole fractions delivered to the analyzer. Since in all our water correction experiments the air stream was in contact with liquid water, the underlying reason may have been dissolution in and outgassing from these reservoirs. This would likely

20   have affected CO_2 more than CH_4, since its solubility in water is much higher. During gas washing bottle experiments, we took this effect into account by carefully observing the equilibration of trace gas mole fraction readings. However, it is conceivable that our efforts were not sufficient. If this explanation were true, the systematic difference between dry air and wet air CO_2 mole fractions in the experiment with Picarro #3 would have precisely compensated for the pressure bend, which seems unlikely. Therefore, we regard this interpretation with caution and acknowledge the possibility that another

25   mechanism caused the inconsistencies of CO_2 readings with the data from the external pressure sensor (a more detailed discussion can be found in Sect. S3). Overall, our results highlight the need for high quality data to correct CO_2 readings for the effects of water vapor.

5 Conclusions

We reported previously rarely detected and unexplained biases of CO_2 and CH_4 measurements obtained with Picarro GHG

30   analyzers in humid air. They were largest at water vapor mole fractions below 0.5 % H_2O, where they amounted to up to 50

% of the WMO inter-laboratory compatibility goal for CH_4, and 80 % for CO_2 in the southern hemisphere at ambient mole fractions. As noted by Stavert et al. (2018), the biases may not only affect measurements without drying systems, but also measurement systems that use Nafion membranes to dry air samples, since the residual water vapor can be in the range of the where the largest biases occurred in our experiments (compare e.g. Verhulst et al., 2017). The biases are due to a sensitivity

5   of the pressure in the measurement cavity to water vapor, which we observed both with an additional external pressure sensor, and based on spectroscopic methods. We speculate that the underlying physical mechanism of the cavity pressure variability is adsorption of water molecules on the piezoresistive pressure sensor in the cavity that is used to keep cavity pressure stable. The biases can be corrected without independent cavity pressure measurements based on experiments with stable water vapor levels by an empirical expansion of the standard water correction model from the literature, which we

10 derived from the cavity pressure dependency on water vapor. Correction of the biases of CO_2 readings was challenging, presumably because of dissolution in and outgassing from the water reservoir we used to humidify the air stream. The commonly used droplet method is not suitable for correcting biases of CO_2 and CH_4 readings related to cavity pressure without independent cavity pressure monitoring, because in these experiments, water vapor can vary faster than it takes cavity pressure to adjust to a new water vapor level. Future research is necessary to understand differences of cavity

15 pressure-related biases of CO_2 and CH_4 between analyzers and over time. Therefore, coefficients for the expanded model should be obtained for each analyzer individually, and be monitored over time.

Accounting for cavity pressure-related biases of CO_2 and CH_4 readings contributes to keeping the overall measurement uncertainty of the widely used Picarro GHG analyzers operated in humid air below the WMO inter-laboratory compatibility goals.

References

30 Chen, H., Winderlich, J., Gerbig, C., Hoefer, A., Rella, C. W., Crosson, E. R., Van Pelt, A. D., Steinbach, J., Kolle, O.,

Beck, V., Daube, B. C., Gottlieb, E. W., Chow, V. Y., Santoni, G. W. and Wofsy, S. C.: High-accuracy continuous airborne measurements of greenhouse gases (CO_2 and CH_4) using the cavity ring-down spectroscopy (CRDS) technique, Atmos. Meas. Tech., 3(2), 375–386, doi:10.5194/amt-3-375-2010, 2010.

Chen, Q., Zhang, M., Liu, S., He, Y., Luo, H., Luo, J. and Lv, W.: Revision to the humidity correction equation in the

5 calculation formulae of the air refractive index based on a phase step interferometer with three frequency-stabilized lasers, Meas. Sci. Technol., 27(12), doi:10.1088/0957-0233/27/12/125002, 2016.

Crosson, E. R.: A cavity ring-down analyzer for measuring atmospheric levels of methane, carbon dioxide, and water vapor, Appl. Phys. B Lasers Opt., 92, 403–408, doi:10.1007/s00340-008-3135-y, 2008.

Johnson, J. E. and Rella, C. W.: Effects of variation in background mixing ratios of N_2, O_2, and Ar on the measurement of

10 $\delta^{18}O$-H_2O and δ^2H-H_2O values by cavity ring-down spectroscopy, Atmos. Meas. Tech. Discuss., 1–39, doi:10.5194/amt-2017-109, 2017.

Kirschke, S., Bousquet, P., Ciais, P., Saunois, M., Canadell, J. G., Dlugokencky, E. J., Bergamaschi, P., Bergmann, D., Blake, D. R., Bruhwiler, L., Cameron-Smith, P., Castaldi, S., Chevallier, F., Feng, L., Fraser, A., Heimann, M., Hodson, E. L., Houweling, S., Josse, B., Fraser, P. J., Krummel, P. B., Lamarque, J.-F., Langenfelds, R. L., Le Quéré, C., Naik, V.,

15 O'Doherty, S., Palmer, P. I., Pison, I., Plummer, D., Poulter, B., Prinn, R. G., Rigby, M., Ringeval, B., Santini, M., Schmidt, M., Shindell, D. T., Simpson, I. J., Spahni, R., Steele, P., Strode, S. A., Sudo, K., Szopa, S., van der Werf, G. R., Voulgarakis, A., van Weele, M., Weiss, R. F., Williams, J. E. and Zeng, G.: Three decades of global methane sources and sinks, Nat. Geosci., 6(10), 813–823, doi:10.1038/ngeo1955, 2013.

McGuire, A. D., Christensen, T. R., Hayes, D., Heroult, A., Euskirchen, E. S., Kimball, J. S., Koven, C. D., Lafleur, P.,

20 Miller, P. A., Oechel, W. C., Peylin, P., Williams, M. R. and Yi, Y.: An assessment of the carbon balance of Arctic tundra: comparisons among observations, process models, and atmospheric inversions, Biogeosciences, 9(8), 3185–3204, doi:10.5194/bg-9-3185-2012, 2012.

Nara, H., Tanimoto, H., Tohjima, Y., Mukai, H., Nojiri, Y., Katsumata, K. and Rella, C. W.: Effect of air composition (N_2, O_2, Ar, and H_2O) on CO_2 and CH_4 measurement by wavelength-scanned cavity ring-down spectroscopy: Calibration and

25 measurement strategy, Atmos. Meas. Tech., 5(11), 2689–2701, doi:10.5194/amt-5-2689-2012, 2012.

Rella, C. W., Chen, H., Andrews, A. E., Filges, A., Gerbig, C., Hatakka, J., Karion, A., Miles, N. L., Richardson, S. J., Steinbacher, M., Sweeney, C., Wastine, B. and Zellweger, C.: High accuracy measurements of dry mole fractions of carbon dioxide and methane in humid air, Atmos. Meas. Tech., 6(3), 837–860, doi:10.5194/amt-6-837-2013, 2013.

Stavert, A. R., Doherty, S. O., Stanley, K., Young, D., Manning, A. J., Mark, F., Rennick, C. and Arnold, T.: UK greenhouse

30 gas measurements at two new tall towers for aiding emissions verification, , , (May), 1–55, 2018.

Verhulst, K. R., Karion, A., Kim, J., Salameh, P. K., Keeling, R. F., Newman, S., Miller, J., Sloop, C., Pongetti, T., Rao, P., Wong, C., Hopkins, F. M., Yadav, V., Weiss, R. F., Duren, R. M. and Miller, C. E.: Carbon dioxide and methane measurements from the Los Angeles Megacity Carbon Project – Part 1: calibration, urban enhancements, and uncertainty estimates, Atmos. Chem. Phys., 17(13), 8313–8341, doi:10.5194/acp-17-8313-2017, 2017.

Winderlich, J., Chen, H., Gerbig, C., Seifert, T., Kolle, O., Lavrič, J. V., Kaiser, C., Höfer, A. and Heimann, M.: Continuous low-maintenance CO_2/CH_4/H_2O measurements at the Zotino Tall Tower Observatory (ZOTTO) in Central Siberia, Atmos. Meas. Tech., 3(4), 1113–1128, doi:10.5194/amt-3-1113-2010, 2010.

WMO: 18th WMO/IAEA Meeting on Carbon Dioxide, Other Greenhouse Gases and Related Tracers Measurement

5   Techniques (GGMT-2015). [online] Available from: https://library.wmo.int/opac/doc_num.php?explnum_id=3074, 2016.